Corresponding States of Structural Glass Formers

Yael S. Elmatad,[1] David Chandler,[1,*] and Juan P. Garrahan[2]

[1]*Department of Chemistry, University of California, Berkeley, CA 94720, USA*
[2]*Department of Physics and Astronomy, University of Nottingham, Nottingham, NG7 2RD, UK*

(Dated: November 25, 2008)

The variation with respect to temperature T of transport properties of 58 fragile structural glass forming liquids (67 data sets in total) are analyzed and shown to exhibit a remarkable degree of universality. In particular, super-Arrhenius behaviors of all super-cooled liquids appear to collapse to one parabola for which there is no singular behavior at any finite temperature. This behavior is bounded by an onset temperature $T_{\rm o}$ above which liquid transport has a much weaker temperature dependence. A similar collapse is also demonstrated, over the smaller available range, for existing numerical simulation data.

Figure 1 shows the collapse of transport data for fragile glass-forming liquids. These refer to super-cooled liquids where the increase of relaxation time τ with decreasing temperature T is more rapid that that of the Arrhenius law, $\log(\tau/\tau_{\rm R}) = E\ (1/T - 1/T_{\rm R})$. Here, $\tau_{\rm R}$ denotes a relaxation time at a reference temperature $T_{\rm R}$, and E stands for activation energy over Boltzmann's constant $k_{\rm B}$. Rather than linear in $1/T$, the collapsed data for $\log\tau$ is quadratic in $1/T$. The data provide no evidence for singular expressions like the Vogel-Fulcher-Tammann (VFT) $\log\tau \sim {\rm const}/(T - T_{\rm K})$ or the mode-coupling $\log\tau \sim {\rm const}|\log(T - T_{\rm c})|$, where $T_{\rm K}$ or $T_{\rm c}$ are finite positive temperatures. These forms are often used to fit transport data of super-cooled liquids [1], and theoretical arguments have been presented as derivations of these forms [2].

This relaxation time τ is an "equilibrium" property. Its value is determined by the thermodynamic state of the system, and nothing more. The rate of preparation, for example, is not pertinent. In contrast, one could consider transport properties when, for example, cooling or warming rates exceed relaxation rates, or at other irreversible conditions like those with which glass is manufactured. In irreversible or driven cases, transport properties can be singular [3]. But in this article, we confine our attention to the reversible case, because it is this case where the great majority of quantitative measurements have been made. It is for this case that we are showing with Figure 1 that there is no evidence of singular behavior controlled by the thermodynamic variable T.

Recently, Dyre and co-workers [4] arrived at a similar conclusion: existing transport data support neither the idea of a finite temperature divergence nor the VFT formula. All the data considered in Ref. [4] and more are treated here. Our analysis takes the further step of collapsing the data and thus demonstrating universality. A similar collapse was noted a few years ago, when Rössler and co-workers showed how seemingly varied behaviors for the transport properties of several super-cooled liquids could be represented by a single function of temperature [5]. The fitting in Figure 1 differs mainly in the functional form adopted for the data collapse. This difference enables a universal fit over a range of temperatures larger than those of Ref. [5]. Kivelson and co-workers [6] have proposed another collapse to a non-singular function, but one with one more adjustable parameter than we consider.

We have used the quadratic form in earlier work [7]. This form could be interpreted in terms of a random energy model, where activation barriers are assumed to be distributed as Gaussian variables [8], but the origin of this distribution would then remain to be explained. We arrived at the quadratic form differently, from a class of kinetically constrained models [9] where the activation energy to relax a domain of length scale ξ grows as $\log\xi$ [10]. The equilibrium domain size is $\xi \simeq c^{-1/d}$, where c is an equilibrium concentration of localized excitations and d is dimensionality. The Boltzmann distribution gives $\log c \propto 1/T$, from which one predicts an activation energy that grows as $1/T$ so that $\log\tau$ grows as $1/T^2$ (to leading order in $1/T$) [10].

We expect the range of validity of this quadratic behavior to be bounded [7]. In particular, it should not apply above a temperature $T_{\rm o}$ where excitations facilitating molecular motions are present throughout the system. In that regime, correlated dynamics is not required for molecular motions, and accordingly, temperature variation of transport is nearly negligible [11]. The quadratic form should also not apply below another temperature, which we call $T_{\rm x}$. The reasoning here recognizes that correlated dynamics leading to super-Arrhenius behavior [12] is the result of constraints due to intermolecular forces. At an energetic cost, E, these constraints can be avoided. The time scale to pay that cost is $\tau_{\rm x}\exp(E/T)$. While this time can be very long, at a low enough temperature it will become shorter than a super-Arrhenius time. This is the temperature $T_{\rm x}$, below which relaxation will be dominated by dynamics that avoid constraints. Therefore, we use

$$\log(\tau/\tau_{\rm o}) \simeq (J/T_{\rm o})^2(T_{\rm o}/T - 1)^2, \quad T_{\rm o} > T > T_{\rm x}\,, \quad (1)$$

to fit data in Figure 1, using J as the parameter to set the energy scale for excitations of correlated dynamics, and

*Electronic address: chandler@cchem.berkeley.edu

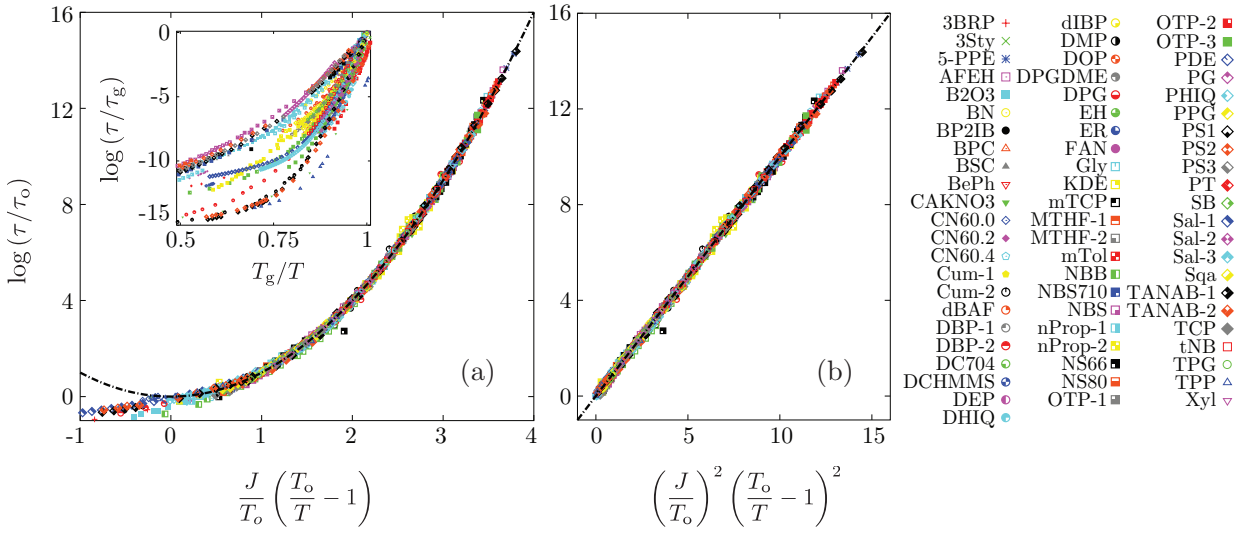

FIG. 1: (a) Collapse to a parabolic form of the structural relaxation times, τ, and viscosities, η, as functions of temperature T for fragile glass forming liquids. Parameters τ_o, T_o and J are listed in Table I. Inset shows the same data when graphed in Angell-type plots, where T_g refers to the temperature at which the viscosity of the liquid is 10^{13} Poise or when the relaxation time reaches 10^2 seconds. (b) Data for temperatures $T < T_o$ graphed as a function of the square of the collapse variable. Key at right lists the 67 liquid data sets considered in the graphs. The meaning of each acronym is given in Table I.

with the understanding that for $T > T_o$, $\log(\tau/\tau_o)$ has little temperature dependence, and for $T < T_x$, $\log(\tau/\tau_o)$ will crossover to Arrhenius temperature dependence.

The onset and crossover temperatures are material properties that may or may not fall within the range of specific experiments. For systems where T_o approaches T_x, fragile behavior will not be observed. Most data that we have found lies in either the fragile and normal liquid regime, $T > T_x$, or in the strong regime, $T < T_x$, but not both. In Ref. [7], we noted published transport data on two organic liquids that appear to exhibit the crossover [13]. But for one of these, salol, other data seem to contradict this finding [14, 38]. Yet a change from super-Arrhenius to Arrhenius behavior should also be reflected in a change of transport de-coupling [15], and this change is seen between dielectric and viscous relaxation [16]. The temperature dependence of transport [17] and of decoupling [18] in films of liquid water also suggest the presence of a crossover. Unfortunately, the amount of data available at present is too sparse to make a convincing case for the origin of this phenomenon. As such, for the present, we focus on the fragile regime.

Table I collects the parameters obtained in the fitting data to Eq.(1) with $T_o > T > T_x$. For each liquid considered, the data set for this regime contained five or more data points, and most contained ten or more data points. This is the data shown in Figure 1. Some of the data refer to viscosity measurements, others refer to relaxation time measurements. We use the same formula for both, replacing τ with η when referring to viscosity. For each liquid, the three fitting parameters are determined by minimizing the mean square deviation, σ^2, between the data and the quadratic form for temperatures that exceed a preliminary estimate of the onset temperature. This estimate is the highest temperature at which the curvature of the data, as a function of $1/T$, appears to take on its maximum value. This estimate usually coincides closely with the value of T_o found from fitting the quadratic form. The standard deviations obtained by this fitting are noted in Table I. Also noted in Table I are the standard deviations obtained by fitting the VFT form to the same data. Both the quadratic form and the VFT form have three independent parameters. Considering all 67 liquid data sets, the mean standard deviation for the parabolic form is 0.073 ± 0.073 and for the VFT form is 0.088 ± 0.14. While the standard deviations are similar, there are at least two reasons to favor the quadratic form over the VFT form. The first [4] is that the quadratic form does not require the introduction of a metaphysical Kauzmann temperature – an implausible thermodynamic state point that by definition is unobservable [19]. The second is that, for approximately half the liquids fitted, the VFT form achieves small standard deviations with a pre-factor time that is less than 10 fs, which is too short to coincide with structural relaxation at any reference state of a molecular liquid.

The reference time, τ_o, is the time for relaxing a microscopic region of liquid at the onset temperature. We expect these times to be significantly larger than 1 ps. Similarly, we expect the reference viscosity, η_o, to be not much smaller than 1 Poise. A much smaller value can be an indication of treating a strong material as if it were fragile. For example, fitting available data for liquid 3-phenyl-1-propanol (3Ph1P) [4, 20] with Eq.(1) yields a seemingly acceptable standard deviation of $\sigma = 0.16$, but the energy scale compared to the reference temperature is curiously

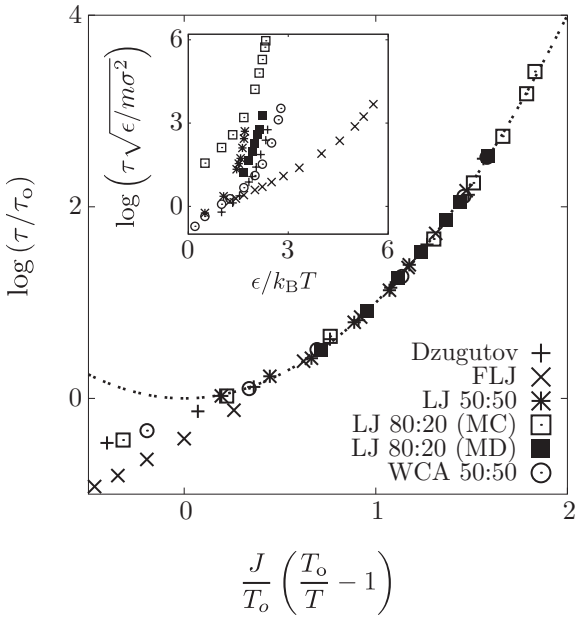

FIG. 2: Collapse to a parabolic form of the structural relaxation times, τ, as functions of temperature T for simulations of models of fragile glass forming liquids. Parameters $\tau_{\rm o}$, $T_{\rm o}$ and J are listed in Table II. Inset shows the same data when graphed as $\log\tau$ vs $1/T$. T is given in units of $\epsilon/k_{\rm B}$ and τ in units of $\sqrt{m\sigma^2/\epsilon}$. Here, m is a particle mass, σ is a particle diameter, and ϵ is an energy parameter that characterizes interparticle interactions. See Refs. [47, 48, 49, 50, 51, 52] for the precise meaning in each particular case. The meaning of each acronym is given in Table II.

low, $J/T_{\rm o} \approx 1.2$, and the reference time is unreasonably short, $\tau_{\rm o} \approx 10^{-16}$ s. Instead, by fitting to the Arrhenius form with $\log(\tau_{\rm R}/{\rm s}) = -2.4$ at $T = T_{\rm R} = 200$K, the activation energy E and standard deviation σ have reasonable values of $40T_{\rm R}$ and 0.57, respectively. Another similar case is the liquid triphenyl-ethylene (TPE) [21]. Again, while the standard deviation $\sigma = 0.0086$ is small, the time is unreasonably short, $\tau_{\rm o} \approx 10^{-14}$ s. An Arrhenius fit for these data yields $\log(\tau_{\rm R}/{\rm s}) = -3.1$, $T_{\rm R} = 274$K, $E/T_{\rm R} = 58$ and $\sigma = 0.058$. The available data therefore suggests that these super-cooled liquids are strong. That is, the crossover temperature is larger than any temperature for which the data is available: $T_{\rm x} > T_R$. Perhaps for these liquids, or others like them, relaxation could be studied at higher temperatures to find evidence for a crossover temperature.

There is one outlying data point on the graphs of Figure 1 for so called NS 66 [22]. This occurs at a state point far separated from all the other state points for which other data points exist. We suspect this point might be erroneous.

Figure 2 shows quadratic data collapse for data from six numerical simulations of fragile glassfomers. Here, the fitting was done using the same methods used to collapse the data in Figure 1(a). Table II shows the parameters used for the data collapse. $J/T_{\rm o}$ for the numerical simulation data is comparable in magnitude to the values obtained for many of the experimental liquids. The simulation data extends over three or four orders of magnitude while the experimental data extends over more than ten orders of magnitude.

Acknowledgments

A number of scientists generously provided data sets that greatly assisted us in this work: L. Berthier, S.-H. Chen, J. Dyre, Y. Gebremichael, T. Hecksher, S. Karmakar, A. S. Keys, L. Maibaum, S. Nagel, R. Richert, S. Sastry, and H. Tanaka. Y. S. E. was supported by NSF GRFP and ONL NDSEG fellowships. D. C. was supported by NSF. J. P. G. was supported by EPSRC grant no. GR/S54074/01. D. C. was Overseas Visiting Scholar of St. John's College, Cambridge during the time that this paper was written.

TABLE I: Fragile Glass Formers

System	Full Name	$T_{\rm o}$/K[a]	$J/T_{\rm o}$[b]	$\log\tau_{\rm o}$/s[c]	$\log\eta_{\rm o}$/P[d]	σ ($\sigma_{\rm VFT}$)[e]	$T_{\rm m}$/K[f]	$T_{\rm g}$/K[g]	Range/K[h]	Ref.
3BRP	3-bromopentane	192	4.3	-9.4		0.13 (0.13)	147	108	107-289	[23]
3Sty	3-styrene	314	8.5	-6.5		0.024 (0.025)	242	237	235-280	[24]
5-PPE	5-polyphenyl-ether	398	6.2	-12.4		0.0044 (0.058)		248	248-264	[21]
AFEH	2-phenyl-5-acetomethyl-5-ethyl-1,3-dioxocylohexane	285	9.4	-6.1		0.0038 (0.0096)		219	220-240	[4]
B2O3	boron oxide (B_2O_3)	1066	3.3		3.0	0.095 (1.0)	723	541	533-1665	[25]
BePh	benzophenone	328	6.3	-11.0		0.05 (0.052)	321	208	215-240	[26]
BN	butyronitrile	135	6.6	-4.8		0.025 (0.021)	116	97	97-116	[27]
BP2IB	biphenyl-2yl-isobutylate	313	6.7	-9.4		0.0063 (0.0084)		209	210-232	[4]
BPC	3,3,4,4,-benzphenonetetra-carboxylicdianhydride	432	9.9	-6.8		0.014 (0.007)		333	334-362	[28]
BSC	Borosilicate Crown glass	2002	2.3		1.9	0.075 (0.15)		825	800-1594	[25]
CaKNO3	Ca-K-NO_3^-	444	10.8		0.3	0.37 (0.22)		338	341-668	[29]
CN60.0	soda lime silicate glass.0	1702	5.2		1.2	0.046 (0.061)		1030	1012-1809	[22]

TABLE I – Continued

System	Full Name	T_o/K[a]	J/T_o[b]	$\log \tau_o$/s[c]	$\log \eta_o$/P[d]	σ (σ_{VFT})[e]	T_m/K[f]	T_g/K[g]	Range/K[h]	Ref.
CN60.2	soda lime silicate glass.2	1668	3.2		1.8	0.086 (0.019)		820	803-1563	[22]
CN60.4	soda lime silicate glass.4	1929	1.9		1.6	0.19 (0.045)		700	684-1563	[22]
Cum-1	isopropyl-benzene	174	8.6	-6.9		0.028 (0.018)	177	129	130-149	[4]
Cum-2	isopropylbenzene	194	6.8		-0.6	0.21 (0.32)	177	129	129-306	[25]
dBAF	dibutyl-ammonium formate	220	6.6	-5.9		0.097 (0.031)		155	156-200	[30]
DBP-1	dibutyl-phtalate	241	8.3	-6.2		0.052 (0.026)	238	179	180-224	[31]
DBP-2	di-n-butylphtalate	320	4.1		-0.9	0.2 (0.36)		168	178-369	[25]
DC704	tetraphenyl-tetramethyl-trisiloxane	306	7.9	-9.8		0.0097 (0.019)		213	211-240	[21]
DCHMMS	dichyclohexyl-methyl-2-methylsuccinate	275	10.9	-5.4		0.0072 (0.0089)		221	220-240	[32]
DEP	diethyl-phtalate	262	7.3	-7.6		0.024 (0.0098)	270	185	186-222	[4, 20]
DHIQ	decahydroisoquinoline	197	25.8	-4.3		0.042 (0.077)		180	180-192	[21]
dIBP	di-iso-butyl-phtalate	247	9.7	-5.4		0.0028 (0.02)		194	195-221	[4]
DMP	dimethyl-phtalate	261	8.5	-6.4		0.017 (0.0077)	275	195	196-220	[4, 20]
DOP	dioctyl-phtalate	251	7.8	-5.1		0.023 (0.0036)	223	187	188-220	[4]
DPG	dipropylene-glycol	268	7.8	-5.9		0.043 (0.021)	<234	196	196-240	[4, 20]
DPGDME	dipropyle-glycol-dimethyl-ether	177	9.9	-6.0		0.015 (0.022)		136	139-155	[4]
EH	ether-2-ethyl-hexylamine	183	9.1	-5.6		0.028 (0.011)	197	140	142-166	[33]
ER	diglycidyl-ether-of-bisphenol A (epoxy-resin)	309	14.0	-6.7		0.014 (0.035)	325	255	259-291	[34]
FAN	3-fluoro-aniline	225	10.3	-7.2		0.16 (0.16)		173	173-198	[35]
Gly	glycerol	338	4.1	-7.7		0.033 (0.0053)	293	191	192-252	[31]
KDE	cresolphthalein-dimethylether	461	7.1	-8.0		0.0095 (0.025)	387	318	315-383	[36]
mTCP	*m*-tricresyl-phosphate	270	9.2	-5.6		0.018 (0.0095)	299	208	209-233	[37]
MTHF-1	2-methyltetrahydrofuran	119	9.8	-6.9		0.022 (0.026)	137	92	91-108	[4]
MTHF-2	2-methyltetrahydrofuran	126	8.5	-8.8		0.049 (0.11)	137	91	94-179	[38]
mTol	*m*-toluene	237	10.6	-6.6		0.01 (0.0051)		185	184-200	[4, 20]
NBB	*n*-butylbenzene	202	5.9		2.0	0.25 (0.16)	185	129	135-306	[25]
NBS	NBS-711 standard	2780	1.1		1.5	0.1 (0.062)		705	665-1614	[25]
NBS 710		2483	1.7		1.5	0.097 (0.018)		830	827-1776	[22]
nProp-1	*n*-propanol	350	1.4	-10.7		0.12 (0.17)	147	99	100-300	[38]
nProp-2	*n*-propanol	398	1.2		-2	0.21 (0.27)	147	99	104-370	[25]
NS 66		2489	1.4		1.2	0.28 (0.19)		726	719-1805	[22]
NS 80		2435	1.5		1.7	0.10 (0.065)		758	718-1759	[22]
OTP-1	*o*-terphenyl	341	8.5	-8.9		0.038 (0.035)	329	243	252-282	[39]
OTP-2	*o*-terphenyl	340	8.6		0.0	0.066 (0.064)	329	240	239-267	[13]
OTP-3	*o*-terphenyl	357	7.7	-9.9		0.16 (0.18)	329	246	248-311	[38]
PDE	phenolphthalein-dimethylether	397	9.3	-7.7		0.022 (0.031)	373	294	299-333	[40]
PG	1,2-propandiol (propylene-glycol)	321	3.4	-7.7		0.0062 (0.0046)	214	164	180-211	[4]
PHIQ	perhydroisoquinoline	208	18.5	-5.8		0.14 (0.055)		181	182-206	[4]
PPG	polypropylene-glycol	263	8.7	-6.1		0.049 (0.0063)	215	199	200-240	[31]
PS1	titania-bearing sodium silicate melt #1	2395	1.7		1.5	0.078 (0.042)		796	837-1591	[41]
PS2	titania-bearing sodium silicate melt #2	2688	1.3		1.3	0.074 (0.038)		746	784-1679	[41]
PS3	titania-bearing sodium silicate melt #3	2109	1.9		1.9	0.081 (0.06)		765	815-1676	[41]
PT	pyridine-toluene	146	17.5	-5.5		0.019 (0.023)		126	125-131	[31]
Sal-1	salol	309	8.1	-8.5		0.05 (0.12)	315	221	218-382	[14]
Sal-2	salol	299	9.1	-8.3		0.066 (0.048)	315	222	223-253	[42]
Sal-3	salol	308	8.3	-8.5		0.069 (0.24)	315	221	220-309	[38]
SB	sucrose-benzonate	421	11.2	-5.8		0.04 (0.019)	373	340	341-400	[43]
Sqa	squalane	224	8.3	-5.3		0.092 (0.053)	235	170	170-210	[21]
TANAB-1	tri-α-naphtylbenzene	519	6.8		-0.9	0.082 (0.34)		335	332-584	[44]
TANAB-2	tri-α-naphtylbenzene	520	6.4		-0.8	0.1 (0.21)		335	333-588	[25]

TABLE I – Continued

System	Full Name	T_o/K[a]	J/T_o[b]	$\log \tau_o$/s[c]	$\log \eta_o$/P[d]	σ (σ_{VFT})[e]	T_m/K[f]	T_g/K[g]	Range/K[h]	Ref.
TCP	tricresyl-phosphate	280	8.8	-6.3		0.012 (0.013)	240	209	216-248	[4, 20]
tNB	trisnaphthylbenzene	510	7.1	-9.2		0.019 (0.023)		342	357-405	[45]
TPG	tripropylene-glycol	251	8.9	-5.5		0.041 (0.0055)	232	192	192-228	[31]
TPP	triphenyl phosphite	286	7.7		-0.5	0.08 (0.18)	296	204	203-291	[46]
Xyl	xylitol	311	11.1	-5.8		0.026 (0.0057)	367	250	254-284	[4]

[a] T_o is the fitted onset temperature in K.
[b] J is the fitted energy scale over k_B.
[c] τ_o is the fitted onset relaxation time in seconds.
[d] η_o is the fitted onset viscosity in Poise.
[e] σ is the standard deviation of the quadratic form given by: $\left(1/(N-n)\sum_i \left(\log_{10}\tau_{fit,i} - \log_{10}\tau_{data,i}\right)^2\right)^{1/2}$. N is the number of fitted data points, $n = 3$ is the number of degrees of freedom for all reported fits. $i = \{1, N\}$ indexes the fitted points. σ_{VFT} is the standard deviation for fitting the parameters τ_o^{VFT}, A and T_K of the VFT form: $\tau = \tau_o^{VFT} \exp\left(A/\left(T - T_K\right)\right)$.
[f] T_m is the melting temperature.
[g] T_g is the glass transition temperature i.e., where $\eta = 10^{13}$ P or $\tau = 10^2$ s.
[h] The range of temperature for data reported in K. Only data for $T < T_o$ is fitted.

TABLE II: Fragile Glass Former Simulations

System	Description	$T_o k_B/\epsilon$[a]	J/T_o[b]	$\log\left(\tau_o/\sqrt{m\sigma^2/\epsilon}\right)$[c]	σ[d]	Range/(k_B/ϵ)[e]	Ref.
Dzugutov	Dzugatov 50:50 Mixture	0.8	1.8	0.3	0.053	0.42-1	[47]
FLJ	Frustrated Lennard-Jones	0.3	1.6	1.5	0.0015	0.18-0.8	[48]
LJ 50:50	Lennard-Jones 50:50 Mixture	0.7	5.6	1.3	0.027	0.59-2	[49]
LJ 80:20 (MC)	Lennard-Jones 80:20 Mixture (Monte Carlo)	0.8	1.9	2.6	0.054	0.43-2	[50]
LJ 80:20 (MD)	Lennard-Jones 80:20 Mixture (Molecular Dynamics)	0.8	1.9	0.7	0.013	0.45-0.6	[51]
WCA 50:50	Weeks-Chandler-Andersen 50:50 Mixture	0.6	2.9	1	0.035	0.36-5	[52]

[a] T_o is the fitted onset temperature in k_B/ϵ
[b] J is the fitted energy scale over k_B.
[c] τ_o is the fitted onset relaxation time in $\sqrt{m\sigma^2/\epsilon}$.
[d] σ is the standard deviation of the quadratic form given by: $\left(1/(N-n)\sum_i \left(\log_{10}\tau_{fit,i} - \log_{10}\tau_{data,i}\right)^2\right)^{1/2}$. N is the number of fitted data points, $n = 3$ is the number of degrees of freedom. $i = \{1, N\}$ indexes the fitted points.
[e] The range of temperature for data reported in units of k_B/ϵ. Only data for $T < T_o$ is fitted.

[1] See for example, M. Ediger, C. Angell, S. Nagel, *J. Phys. Chem.* **100**, 13200 (1996).
[2] See for example, G. Adam, J. H. Gibbs, *J. Chem. Phys.* **43**, 139 (1965); W. Götze and L. Sjögren, *Rep. Prog. Phys.* **55**, 55 (1992); M. Mézard and G. Parisi, *Phys. Rev. Lett.* **82**, 747 (1999); W. Götze, *J. Phys. Condens. Matter* **11**, 10A (1999); X. Xia, P. G. Wolynes, *Phys. Rev. Lett.* **86**, 5526 (2001); J. P. Bouchaud and G. Biroli, *J. Chem. Phys.* **121**, 7347 (2004).
[3] See for example, M. Sellitto, J. Kurchan, *Phys. Rev. Lett.* **95**, 236001 (2005); M. Merolle, J. P. Garrahan, D. Chandler, *Proc. Nat. Acad. Sci.* **102**, 10837 (2005); J. P. Garrahan, *et al.*, *Phys. Rev. Lett.* **98**, 195702 (2007).
[4] T. Hecksher, *et al.*, *Nat. Phys.* **4**, 737 (2008).
[5] E. Rössler, K.-U. Hess, V. Novikov, *J. Non-Cryst. Solids.* **223**, 207 (1998).
[6] D. Kivelson, S. A. Kivelson, X. Zhao, Z. Nussinov and G. Tarjus, *Physica A* **219**, 27 (1995); D. Kivelson, G. Tarjus, X. Zhao, and S. A. Kivelson, *Phys. Rev. E* **53**, 751 (1996).
[7] J. Garrahan, D. Chandler, *Proc. Nat. Acad. Sci.* **100**, 9710 (2003).

[8] H. Bässler, *Phys. Rev. Lett.* **58**, 767 (1987).
[9] G. Fredrickson, H. Andersen, *Phys. Rev. Lett.* **53**, 1244 (1984); F. Rirtort, P. Sollich. *Adv. Phys.* **52**, 219 (2003).
[10] P. Sollich and M. R. Evans, *Phys. Rev. Lett.* **83**, 3238 (1999); D. Aldous and P. Diaconis, *J. Stat. Phys.* **107**, 945 (2002); L. Berthier and J. P. Garrahan, *J. Phys. Chem. B* **109**, 3578 (2005); D. J. Ashton, L. O. Hedges and J. P. Garrahan, *J. Stat. Mech.* P12010 (2005); N. Cancrini, *et al.*, arXiv:0712.1934 (2007).
[11] D. Chandler, J. D. Weeks, H. C. Andersen, *Science* **220**, 787 (1983); J. Jonas, *Science* **216**, 1179 (1982).
[12] R. G. Palmer, *et al.*, *Phys. Rev. Lett* **53**, 958 (1984).
[13] W. T. Laughlin, D. R. Uhlmann, *J. Phys. Chem.* **76**, 2317 (1972).
[14] P. Dixon, N. Menon, S. Nagel, *Phys. Rev. E* **50**, 1717 (1994).
[15] A. Pan, D. Chandler, J. P. Garrahan, *ChemPhysChem* **6**, 1783 (2005).
[16] I. Chang, H. Sillescu, *J. Phys. Chem. B* **101**, 8794 (1997).
[17] L. Liu, *et al.*, *Phys. Rev. Lett.* **95**, 117802 (2005).
[18] S.-H. Chen, *et al.*, *Proc. Nat. Acad. Sci.* **103**, 9012 (2006).
[19] F. H. Stillinger, *J. Chem. Phys.* **88**, 7818 (1988).
[20] B. Igarashi, *et al.*, *Rev. Sci. Instrum.* **79**, 045105 (2008); B. Igarashi, *et al.*, *Rev. Sci. Instrum.* **79**, 045106 (2008).
[21] B. Jakobsen, K. Niss, N. B. Olsen, *J. Chem. Phys.* **123**, 234511 (2005).
[22] D. R. Neuville, *Chem. Geo.* **229**, 28 (2006).
[23] J. G. Berberian, R. H. Cole, *J. Chem. Phys.* **84**, 6921 (1986).
[24] T. Blochowicz, Ph.D. thesis, Universitat Bayreuth (2003).
[25] H. Tweer, J. H. Simmons, P. B. Macedo, *J. Chem. Phys.* **54**, 1952 (1971).
[26] P. Lunkenheimer, *et al.*, *Phys. Rev. E* **77**, 031506 (2008).
[27] N. Ito, *et al.*, *J. Chem. Phys.* **125**, 024504 (2006).
[28] K. L. Ngai, M. Paluch, *J. Chem. Phys.* **120**, 857 (2004).
[29] C. A. Angell, *J. Non-Cryst. Solids* **102**, 205 (1988).
[30] N. Ito, W. Huang, R. Richert, *J. Phys. Chem. B* **110**, 4371 (2006).
[31] N. B. Olsen, T. Christensen, J. C. Dyre, *Phys. Rev. Lett.* **86**, 1271 (2001).
[32] R. Diaz-Calleja, *et al.*, *Phys. Rev. E* **72**, 051505 (2005).
[33] L.-M. Wang, R. Richert, *J. Phys. Chem. B* **109**, 11091 (2005).
[34] M. Mierzwa, *et al.*, *J. Chem. Phys.* **128**, 044512 (2008).
[35] J. Wiedersich, *et al.*, *J. Phys.: Condens. Matter* **11**, A147 (1999).
[36] M. Paluch, K. L. Ngai, S. Hensel-Bielowka, *J. Chem. Phys.* **114**, 10872 (2001).
[37] T. Blochowicz, *et al.*, *J. Chem. Phys.* **124**, 134503 (2006).
[38] R. Richert, C. A. Angell, *J. Chem. Phys.* **108**, 9016 (1998).
[39] R. Richert, *J. Chem. Phys.* **123**, 154502 (2005).
[40] S. Hensel-Bielowka, M. Paluch, *Phys. Rev. Lett.* **89**, 025704 (2002).
[41] M. Liska, *et al.*, *Chem. Geo.* **128**, 199 (1996).
[42] C. Gainaru, *et al.*, *Phys. Rev. B.* **72**, 174203 (2005).
[43] J. R. Rajian, *et al.*, *J. Chem. Phys.* **124**, 014510 (2006).
[44] D. J. Plazek, J. H. Magill, *J. Chem. Phys.* **45**, 3038 (1966).
[45] R. Richert, K. Duvvuri, L.-T. Duong, *J. Chem. Phys.* **118**, 1828 (2003).
[46] L. M. Martinez, C. A. Angell, *Nature* **410**, 663 (2001).
[47] Y. Gebremichael, Ph.D. thesis, University of Michigan (2004).
[48] H. Shintani, H. Tanaka, *Nat. Mater.* **7**, 870 (2008).
[49] N. Lacevic, *et al.*, *J. Chem. Phys.* **119**, 7372 (2003).
[50] L. Berthier, W. Kob, *J. Phys.: Condens. Matter* **19**, 205130 (2007).
[51] S. Karmakar, C. Dasgupta, S. Sastry, arXiv.org:0805.3104 (2008).
[52] L. O. Hedges, *et al.*, *J. Chem. Phys.* **127**, 211101 (2007).